Food Science of Animal Resources

Food Sci. Anim. Resour. 2021 September 41(5):802~815
DOI https://doi.org/10.5851/kosfa.2021.e37

pISSN : 2636-0772 eISSN : 2636-0780
http://www.kosfaj.org

ARTICLE

Effect of Postmortem Phases on Lamb Meat Quality: A Physicochemical, Microstructural and Water Mobility Approach

Yue Ge, Dequan Zhang, Huimin Zhang, Xin Li, Fei Fang, Ce Liang, and Zhenyu Wang*

Institute of Food Science and Technology, Chinese Academy of Agricultural Sciences, Key Laboratory of Agro-Products Quality and Safety Control in Storage and Transport Process, Ministry of Agriculture and Rural Affairs, Beijing 100193, China

OPEN ACCESS

Received May 28, 2021
Revised July 6, 2021
Accepted July 26, 2021

*Corresponding author : Zhenyu Wang
Institute of Food Science and Technology, Chinese Academy of Agricultural Sciences, Key Laboratory of Agro-Products Quality and Safety Control in Storage and Transport Process, Ministry of Agriculture and Rural Affairs, Beijing 100193, China
Tel: +86-10-62818740
Fax: +86-10-62818740
E-mail: caasjgsmeat2021_1@126.com

*ORCID
Yue Ge
https://orcid.org/0000-0002-0214-9541
Dequan Zhang
https://orcid.org/0000-0003-3277-6113
Huimin Zhang
https://orcid.org/0000-0002-3713-0656
Xin Li
https://orcid.org/0000-0001-7924-6449
Fei Fang
https://orcid.org/0000-0001-6640-804X
Ce Liang
https://orcid.org/0000-0003-2859-2610
Zhenyu Wang
https://orcid.org/0000-0003-4478-1710

Abstract To investigate the effect of postmortem phases on lamb meat quality, the physicochemical quality, microstructure and water mobility of oyster cut, short loin, knuckle and silverside muscles from Small-Tail Han sheep were evaluated in the pre-rigor, rigor mortis and post-rigor phases. Pre-rigor lamb meat had higher pH and water holding capacity (WHC), whereas lower CIE L*, b*, hue angle values than rigor mortis and post-rigor meat ($p<0.05$). The Warner-Bratzler shear force (WBSF) values were higher in rigor mortis short loin and silverside than their pre-rigor and post-rigor counterparts, pre-rigor short loin had lower WBSF value than its post-rigor counterpart ($p<0.05$). Muscle fibers shrank laterally and longitudinally during the onset of rigor mortis. Rigor mortis and post-rigor lamb meat exhibited wide I-bands, dark A-bands, short sarcomeres and large inter-myofibrillar spaces. The shift of immobilized water to free water and repulsion from the intra-myofibrillar space to the extracellular space result in the increase of water loss in rigor mortis and post-rigor lamb meat. The results of the principal component analysis (PCA) indicated that rigor mortis and post-rigor lamb meat had similar quality properties but different from pre-rigor lamb meat. In conclusion, the lamb meat in the pre-rigor phase had good tenderness, color and WHC. The results of this research could provide some theoretical references for lamb meat production and processing.

Keywords lamb meat quality, pre-rigor, rigor mortis, post-rigor, microstructure

Introduction

Lamb meat is one of the most popular meat in many countries of the world, and the consumption of lamb meat is increasing globally (Suleman et al., 2020). The consumption patterns of lamb meat are very diverse in different regions around the world (Nam et al., 2010). In the USA, Australia and other Western places, the commercial abattoirs commonly use chilling procedure to produce aged lamb meat, with aging time commonly from 5 to 28 d and even longer (Colle et al., 2016; Geesink

et al., 2011; Kim et al., 2018; Xiao et al., 2020). However, consumers in some Eastern countries, such as China, prefer pre-rigor meat, which is ubiquitous in Chinese commercial abattoirs (Xiao et al., 2020). Without aging process, pre-rigor meat requires less cooler space, electricity consumption and capital investment (Lang et al., 2016; Sukumaran et al., 2018).

The conversion of muscle to meat and subsequent aging involve complex energy metabolism, biochemical and physiological changes, including the pre-rigor, rigor mortis and post-rigor phases (Lawrie and Ledward, 2017; Xiao et al., 2020). Generally, the pH of lamb muscle declines to ultimate pH at 24 h postmortem, with the muscle fibers enter rigor and the muscle stiffness occurs, complete rigor mortis was attained (Lawrie and Ledward, 2017). During subsequent aging process, with the degradation of cytoskeletal proteins and the increase of sarcomere length, the muscle tension decreased (resolution of rigor mortis) (Lawrie and Ledward, 2017). Xiao et al. (2020) reported that before 12 h postmortem the lamb topside muscle was in the pre-rigor phase, 12–24 h postmortem was in the rigor mortis phase, 3–7 d postmortem was in the post-rigor phase according to the pH and Warner-Bratzler shear force (WBSF) values.

The process of rigor mortis and resolution of muscle could affect the meat quality significantly (Lawrie and Ledward, 2017; Xiao et al., 2020). Wheeler and Koohmaraie (1994) reported that the WBSF of ovine *longissimus* muscle increased from 5.10 kg at 3 h postmortem (per-rigor) to 8.66 kg at 24 h postmortem (rigor mortis), and then decreased to 4.36 kg by 72 h postmortem (post-rigor). Wu et al. (1995) found that pre-rigor bovine *stemomandibularis* muscle was more tender than post-rigor control muscle cooked to 70℃ internally. The amount of free water increased during rigor mortis and resolution, which caused an accumulation of water on the cut surface and higher drip loss (Devine et al., 2014). Meat tenderness, color and water holding capacity (WHC) are main quality traits concerned by consumers and meat industry (Li et al., 2021). To date, the quality properties of rigor mortis and post-rigor meat have been systematically investigated (Colle et al., 2016; Lawrie and Ledward, 2017; Pearce et al., 2011). However, little is known about the quality properties of per-rigor lamb meat. Therefore, the aim of this research was to investigate the physicochemical quality and microstructure of pre-rigor (45 min postmortem), rigor mortis (24 h postmortem) and post-rigor (72 h postmortem) lamb meat, and the principal component analysis (PCA) method were used to compare and analyze the differences of quality properties of lamb meat in different stages of postmortem.

Materials and Methods

Animals and cuts collection

Fifty-four male sheep carcasses (8 mon of age, Small-Tail Han sheep) with the same feeding system (drylot feeding with the same commercial diet) were randomly collected at a local commercial abattoir in Hebei, China. The Small-Tail Han sheep is a predominant local sheep variety and widely raised in many provinces of China, which originated from Mongolia Sheep and carefully cultivated for a long time in northern China (Li et al., 2018). The 54 carcasses were allocated randomly to three groups for sampling in pre-rigor (45 min postmortem), rigor mortis (24 h postmortem) and post-rigor (72 h postmortem) with 18 carcasses in each group. All of the carcasses were hot-deboned, about 200 g of meat sample was obtained from the oyster cut (a mixture of *subscapularis, infraspinatus, teres minor* and *supraspinatus*), short loin (*longissimus thoracis et lumborum*), knuckle (*quadriceps femoris*) and silverside (a mixture of *biceps femoris* and *semitendinosus*) in the right side of the lamb carcasses immediately after slaughter. After trimming the external fat and connective tissue, each sample was dissected into two sections. One section was wrapped in polyethylene cling film and placed in a chiller (~4℃) used for pH, color and microstructure analysis; the other section was vacuum packed (the average packaged weight was 128.63±8.28 g), frozen (at

45 min postmortem or after refrigerating at 4℃ for 24 or 72 h) and stored at –35℃ for further WHC and WBSF measurements.

pH measurement

The pH measurement was preformed using a portable pH meter (Testo 205, Testo, Lenzkirch, Germany). The glass probe of the pH meter was directly inserted into the center of the samples after calibrating with pH 4.00 and pH 7.00 standard buffers. For each sample, four measurements were made at different positions, and the average value was used for further analysis.

Color measurement

The cut surface was exposed in the air for 30–40 min at ~4℃ to allow blooming prior to color determination. The color analysis was conducted by a portable colorimeter (Minolta CR-400, Konica Minolta Optics, Osaka, Japan) according to Calnan et al. (2016). The lightness (CIE L*), redness (CIE a*) and yellowness (CIE b*) of the samples were recorded, and the parameters hue angle and Chroma were calculated by the equations $\tan^{-1}(b^*/a^*)$ and $\sqrt{a^{*2}+b^{*2}}$, respectively.

Water holding capacity (WHC) analysis

Thawing loss

Frozen samples (128.63±8.28 g) were thawed at 4℃ for 16 h, thawing loss (TL) was expressed as a percentage of weight loss before and after thawing (Li et al., 2012).

Cooking loss and total moisture loss

The cooking loss (CL) of the samples was determined according to the procedure described by Hopkins et al. (2010). Briefly, thawed samples were dissected into blocks with the weight of 65 g, placed inside polyethylene bags and cooked for 35 min in 71℃ water-bath. CL was expressed as a percentage of weight loss before and after cooking. Total moisture loss (TML) was the sum of TL and CL.

Low-field nuclear magnetic resonance (LF-NMR) analysis

^{1}H NMR transverse relaxation times (T_{2b}, T_{21}, T_{22}) and their corresponding water populations (P_{2b}, P_{21}, P_{22}) measurements were conducted on an NMR analyzer (NM120-040H-1, Niumag Electric, Shanghai, China) by using the Carr-Purcell-Meiboom-Gill (CPMG) sequences (Li et al., 2014). After thawed at 4℃ for 16 h, the samples were cut into 3×1×1 cm parallel to the orientation of muscle fiber, placed in a plastic tube and inserted into the NMR probe. The analysis was performed at 32℃. The spectrometer frequency was 20 MHz, and the τ value (time between 90° pulse and 180° pulse) was 100 μs. The repetition time between the two succeeding scans was 1,500 ms. Data were acquired as 8 scan repetitions for each sample. The data were expressed by using the software of MultiExp Invert Analysis 4.6 (Niumag Electric).

Warner-Bratzler shear force (WBSF) measurement

The WBSF measurement was preformed using a texture analyzer (TA-XT plus, Stable Micro System, UK) equipped with

an HDP/BSW probe. Briefly, after CL determination, the samples were cooled at 4°C overnight, and each sample was cut into 6 to 8 cubes (1 cm^2 cross section) parallel to the orientation of muscle fiber and sheared by the texture analyzer. The average peak force of the subsamples was calculated and the shear force was expressed as N/cm^2.

Muscle microstructure analysis

Scanning electron microscope (SEM)

The meat samples in different stages of postmortem were dissected into 2×2×3 mm parallel to the orientation of muscle fiber and fixed overnight in 2.5% glutaraldehyde, then rinsed for 1 h with distilled water and dehydrated with graded ethanol. Dried samples were sputter-coated with gold and observed with SEM (SU8010, Hitachi, Tokyo, Japan) at a magnification of 500× (Qian et al., 2020).

Transmission electron microscope (TEM)

The samples were cut into 1×1×3 mm and fixed overnight in 2.5% glutaraldehyde, then post-fixed with 1% OsO_4 and washed with 0.1 M phosphate buffer, followed by dehydration in ethanol. After embedded in spur resin, meat sections were prepared using the Leica ultramicrotome, and then stained with uranyl acetate and lead citrate and observed under TEM (H-7500, Hitachi) at a magnification of 15,000× (Lang et al., 2016). The pictures were analyzed by using the software of Image-Pro Plus 6.0 (Media Cybernetics, Rockville, MD, USA).

Statistical analysis

The data analyses were conducted using SPSS 25.0 (IBM, Chicago, IL, USA) and Origin 2021b software (OriginLab, Northampton, MA, USA). The mean values of the variables were analysed by one-way ANOVA and Duncan-multiple range test, least significant differences ($p<0.05$) were reported. The postmortem phases and cuts were considered as the fixed effects, and animals as the random effect. The PCA of the variables were done by the PCA package of Origin.

Results

pH

As shown in Table 1, the pH of lamb oyster cut, short loin, knuckle and silverside declined from 6.50–6.58 in pre-rigor to 5.63–5.92 in rigor mortis ($p<0.05$), and then remained stable from rigor mortis to post-rigor ($p>0.05$). Short loin (5.63) and silverside (5.64) had lower ultimate pH than oyster cut (5.86) and knuckle (5.92) at 24 h postmortem ($p<0.05$).

Color

The L*, b* and hue angle values were significantly higher in rigor mortis and post-rigor cuts than their pre-rigor counterparts ($p<0.05$, Table 1). Pre-rigor meat had lower a* value than rigor mortis meat in the four cuts ($p<0.05$), whereas pre-rigor and post-rigor meat had similar a* value in short loin and silverside cuts ($p>0.05$).

Water holding capacity (WHC)

As shown in Table 2, rigor mortis cuts had the highest TL, followed by post-rigor cuts, whereas pre-rigor cuts had the

Table 1. pH and color values of lamb oyster cut, short loin, knuckle and silverside in the pre-rigor, rigor mortis and post-rigor phases

Parameters	Postmortem phases	Cuts			
		Oyster cut	Short loin	Knuckle	Silverside
pH	Pre-rigor	6.50±0.20^{Aa}	6.54±0.16^{Aa}	6.53±0.20^{Aa}	6.58±0.18^{Aa}
	Rigor mortis	5.86±0.13^{Ba}	5.63±0.10^{Bb}	5.92±0.17^{Ba}	5.64±0.07^{Bb}
	Post-rigor	5.96±0.27^{Ba}	5.63±0.11^{Bb}	5.88±0.17^{Ba}	5.69±0.13^{Bb}
CIE L*	Pre-rigor	31.60±1.74^{Ca}	28.01±1.28^{Bc}	30.10±1.56^{Bb}	27.57±1.52^{Bc}
	Rigor mortis	37.95±2.17^{Ba}	35.48±1.73^{Ab}	35.91±2.11^{Ab}	34.99±1.76^{Ab}
	Post-rigor	39.44±1.82^{Aa}	36.36±1.72^{Abc}	37.08±2.18^{Ab}	35.29±1.42^{Ac}
CIE a*	Pre-rigor	13.30±1.20^{Ba}	12.15±10.03^{Bb}	12.53±1.51^{Bab}	12.53±1.11^{Bab}
	Rigor mortis	14.78±10.09^{Aa}	13.17±0.95^{Ab}	14.79±1.33^{Aa}	14.20±1.33^{Aa}
	Post-rigor	14.81±1.32^{Aa}	12.50±0.94^{ABb}	14.67±1.80^{Aa}	12.31±0.85^{Bb}
CIE b*	Pre-rigor	2.20±0.51^{Ca}	1.77±0.41^{Cb}	1.94±0.51^{Cab}	1.91±0.39^{Cab}
	Rigor mortis	4.91±0.57^{Bb}	4.85±0.57^{Bb}	4.84±0.95^{Bb}	5.58±0.68^{Ba}
	Post-rigor	7.02±0.91^{Aa}	6.72±0.80^{Aa}	6.81±0.97^{Aa}	6.90±0.43^{Aa}
Hue angle	Pre-rigor	9.49±1.50^{Ca}	7.64±2.34^{Cb}	8.73±1.42^{Cab}	8.21±1.00^{Cab}
	Rigor mortis	18.31±1.80^{Bb}	21.64±1.73^{Ba}	16.90±1.64^{Bc}	21.29±1.90^{Ba}
	Post-rigor	26.53±2.31^{Ab}	29.19±1.84^{Aa}	23.19±2.07^{Ac}	29.15±1.85^{Aa}
Chroma	Pre-rigor	13.34±1.13^{Ba}	12.14±0.95^{Bb}	12.84±1.48^{Cab}	12.51±0.97^{Cab}
	Rigor mortis	15.51±0.97^{Aa}	13.88±1.44^{Ab}	15.46±1.46^{Ba}	15.42±1.31^{Aa}
	Post-rigor	15.75±1.12^{Ab}	13.83±1.23^{Ac}	16.95±1.60^{Aa}	14.18±0.99^{Bc}

Data were recorded as mean±SD.
$^{A–C}$ Means with different letters indicate significant difference ($p<0.05$) between postmortem phases in the same cut.
$^{a–c}$ Means with different letters indicate significant difference ($p<0.05$) between cuts in the same postmortem phase.

lowest TL ($p<0.05$). The TL of rigor mortis cuts (oyster cut, 4.02%; short loin, 8.21%; knuckle, 3.18%; silverside, 6.14%) were almost twice as much as their pre-rigor counterparts (2.31%, 4.11%, 1.73%, and 3.79%, respectively). Similarly, compare with rigor mortis cuts, pre-rigor cuts also had less TML ($p<0.05$), there was no significant difference of CL between pre-rigor and rigor mortis cuts ($p>0.05$).

Pre-rigor cuts had higher NMR T_2 relaxation time of immobilized water (T_{21}) compared with rigor mortis cuts ($p<0.05$), and the T_{21} of pre-rigor short loin, knuckle and silverside were higher than those of post-rigor cuts ($p<0.05$). The proton populations of immobilized water (P_{21}) in short loin and silverside decreased by 0.26% and 0.79%, meanwhile, the proton population of free water (P_{22}) in short loin increased by 0.51% during the onset of rigor mortis ($p<0.05$).

Warner-Bratzler shear force (WBSF)

As shown in Fig. 1, WBSF values were higher in rigor mortis meat than in pre-rigor and post-rigor meat for all cuts except oyster cut ($p<0.05$). For short loin, pre-rigor meat had lower WBSF than post-rigor meat (pre-rigor, 58.10 N; post-rigor, 69.49 N; $p<0.05$). However, for other cuts no different were found between pre-rigor and post-rigor meat ($p>0.05$). Oyster cut had the lowest WBSF values than other cuts in different stages of postmortem ($p<0.05$).

Table 2. Thawing loss, cooking loss, total moisture loss, NMR T_2 relaxation times (T_{2b}, T_{21}, and T_{22}) and corresponding proton populations (P_{2b}, P_{21}, and P_{22}) of lamb oyster cut, short loin, knuckle and silverside in the pre-rigor, rigor mortis and post-rigor phases

Parameters	Postmortem phases	Cuts			
		Oyster cut	Short loin	Knuckle	Silverside
Thawing loss (%)	Pre-rigor	2.31±0.60^{Bb}	4.11±0.77^{Ca}	1.73±0.53^{Bb}	3.79±0.63^{Ba}
	Rigor mortis	4.02±0.56^{Ac}	8.21±0.91^{Aa}	3.18±0.74^{Ad}	6.14±0.87^{Ab}
	Post-rigor	2.18±0.66^{Bc}	5.91±1.44^{Ba}	2.11±0.79^{Bc}	4.36±0.85^{Bb}
Cooking loss (%)	Pre-rigor	28.93±1.86^{Aa}	27.28±1.27^{Bb}	28.98±2.00^{Aa}	27.40±2.34^{Bb}
	Rigor mortis	30.07±2.07^{Aa}	28.25±1.57^{Bb}	29.93±20.08^{Aa}	28.95±1.92^{ABab}
	Post-rigor	30.29±2.42^{Aab}	31.15±2.11^{Aa}	30.34±2.72^{Aab}	29.21±2.28^{Ab}
Total moisture loss (%)	Pre-rigor	32.04±2.07^{Ba}	31.75±2.21^{Ba}	30.88±2.56^{Aa}	30.68±2.60^{Ca}
	Rigor mortis	34.39±2.91^{Ab}	36.57±2.30^{Aa}	32.18±2.59^{Ac}	35.44±2.48^{Aab}
	Post-rigor	32.54±2.59^{Bb}	37.29±2.34^{Aa}	32.16±2.66^{Ab}	33.34±2.60^{Bb}
T_{2b} (ms)	Pre-rigor	0.39±0.10^{Bab}	0.34±0.07^{Abc}	0.30±0.07^{Bc}	0.42±0.09^{Aa}
	Rigor mortis	0.50±0.15^{Aa}	0.38±0.12^{Ab}	0.43±0.18^{Aab}	0.36±0.10^{Ab}
	Post-rigor	0.46±0.09^{ABa}	0.37±0.11^{Aa}	0.37±0.10^{ABa}	0.46±0.19^{Aa}
T_{21} (ms)	Pre-rigor	54.74±2.81^{Aa}	49.57±1.66^{Ac}	54.78±2.72^{Aa}	51.48±2.47^{Ab}
	Rigor mortis	50.60±2.95^{Ba}	44.80±2.79^{Bc}	50.72±1.63^{Ba}	47.64±2.45^{Bb}
	Post-rigor	54.06±3.13^{Aa}	46.17±2.96^{Bd}	51.60±2.72^{Bb}	49.46±1.98^{Bc}
T_{22} (ms)	Pre-rigor	314.97±26.93^{Ca}	267.94±15.48^{Ac}	299.26±22.69^{Bb}	289.63±19.76^{Ab}
	Rigor mortis	336.17±21.13^{Bb}	276.25±19.75^{Ad}	365.59±45.68^{Aa}	302.19±12.88^{Ac}
	Post-rigor	366.20±27.49^{Aa}	271.92±22.34^{Ac}	361.19±26.80^{Aa}	299.81±22.27^{Ab}
P_{2b} (%)	Pre-rigor	4.80±0.72^{Ab}	5.61±0.57^{Aa}	4.86±0.48^{Ab}	5.19±0.80^{Aab}
	Rigor mortis	4.09±0.51^{Bb}	5.14±0.89^{Aa}	4.44±0.65^{ABb}	5.04±0.90^{Aa}
	Post-rigor	4.00±0.34^{Ba}	4.18±1.41^{Ba}	4.08±0.62^{Ba}	4.22±0.84^{Ba}
P_{21} (%)	Pre-rigor	93.23±0.69^{Aa}	92.23±0.47^{Ab}	92.94±0.83^{Aa}	92.83±0.81^{Aa}
	Rigor mortis	92.77±0.82^{Aa}	91.97±0.51^{Bb}	93.05±1.05^{Aa}	92.04±0.73^{Bb}
	Post-rigor	94.41±0.78^{Aa}	92.68±0.73^{Ac}	93.71±0.71^{Ab}	92.95±0.69^{Ad}
P_{22} (%)	Pre-rigor	2.28±0.64^{Aa}	2.22±0.53^{Ba}	2.25±0.89^{Aa}	2.26±0.97^{Aa}
	Rigor mortis	2.39±0.77^{Aa}	2.73±0.72^{Aa}	2.38±10.01^{Aa}	2.58±0.90^{Aa}
	Post-rigor	1.44±0.38^{Bb}	1.95±0.52^{Ba}	1.76±0.79^{Aab}	2.15±0.61^{Aa}

Data were recorded as mean±SD.
$^{A–C}$ Means with different letters indicate significant difference ($p<0.05$) between postmortem phases in the same cut.
$^{a–c}$ Means with different letters indicate significant difference ($p<0.05$) between cuts in the same postmortem phase.
NMR, nuclear magnetic resonance.

Micro- and ultra-structure

Micro- and ultra-structure of the lamb samples in the pre-rigor, rigor mortis and post-rigor phases are showed in Fig. 2 and 3. Compared to pre-rigor cuts, significant shrinkage of muscle fibers and the gaps formation among muscle fibers can be seen in rigor mortis and post-rigor cuts (Fig. 2). From pre-rigor to post-rigor, the diameters of muscle fiber of oyster cut, short loin, knuckle and silverside decreased from 33.30, 37.60, 34.36, and 44.91 μm to 29.34, 28.1, 27.24, and 30.64 μm, respectively

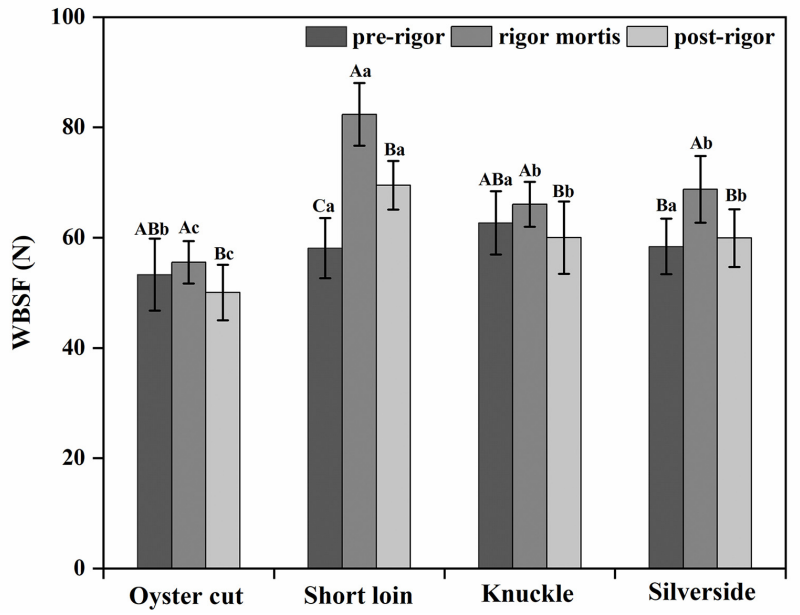

Fig. 1. Warner-Bratzler shear force (WBSF) values of lamb oyster cut, short loin, knuckle and silverside in the pre-rigor, rigor mortis and post-rigor phases. Data were recorded as mean±SD. $^{A–C}$ Means with different letters indicate significant difference ($p<0.05$) between postmortem phases in the same cut. $^{a–c}$ Means with different letters indicate significant difference ($p<0.05$) between cuts in the same postmortem phase.

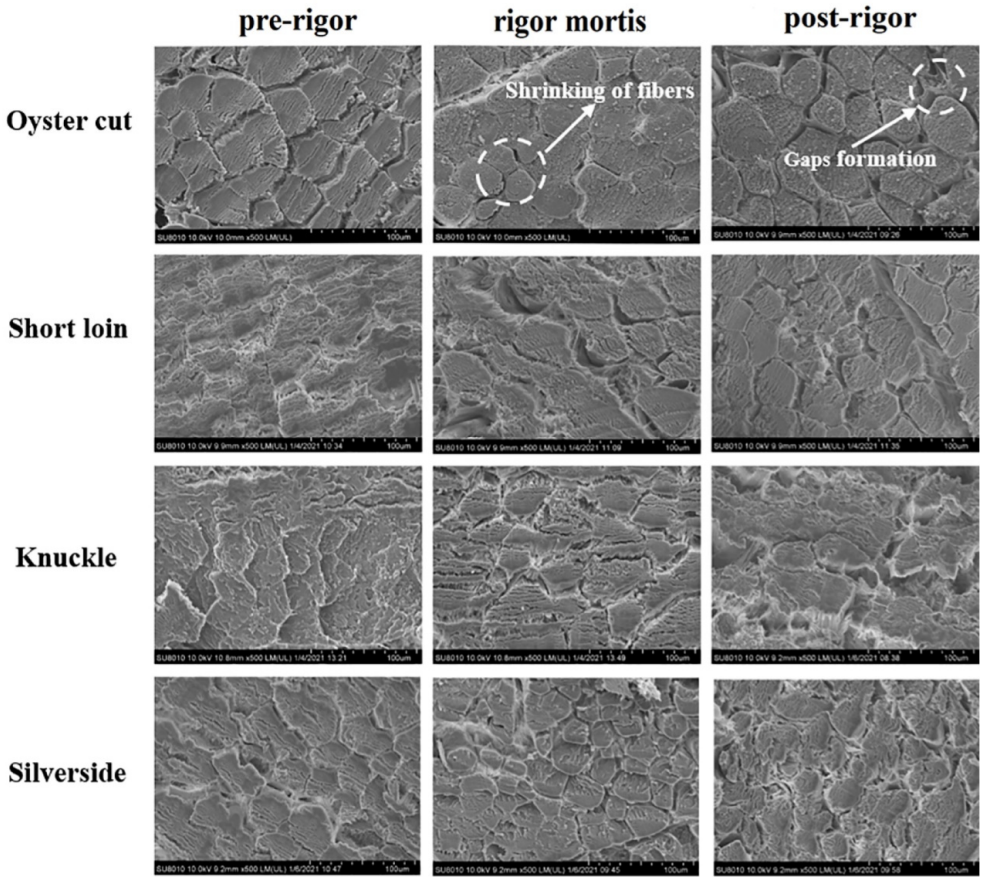

Fig. 2. Scanning electron micrographs of lamb oyster cut, short loin, knuckle and silverside in the pre-rigor, rigor mortis and post-rigor phases (500×). Scale bar=100 μm.

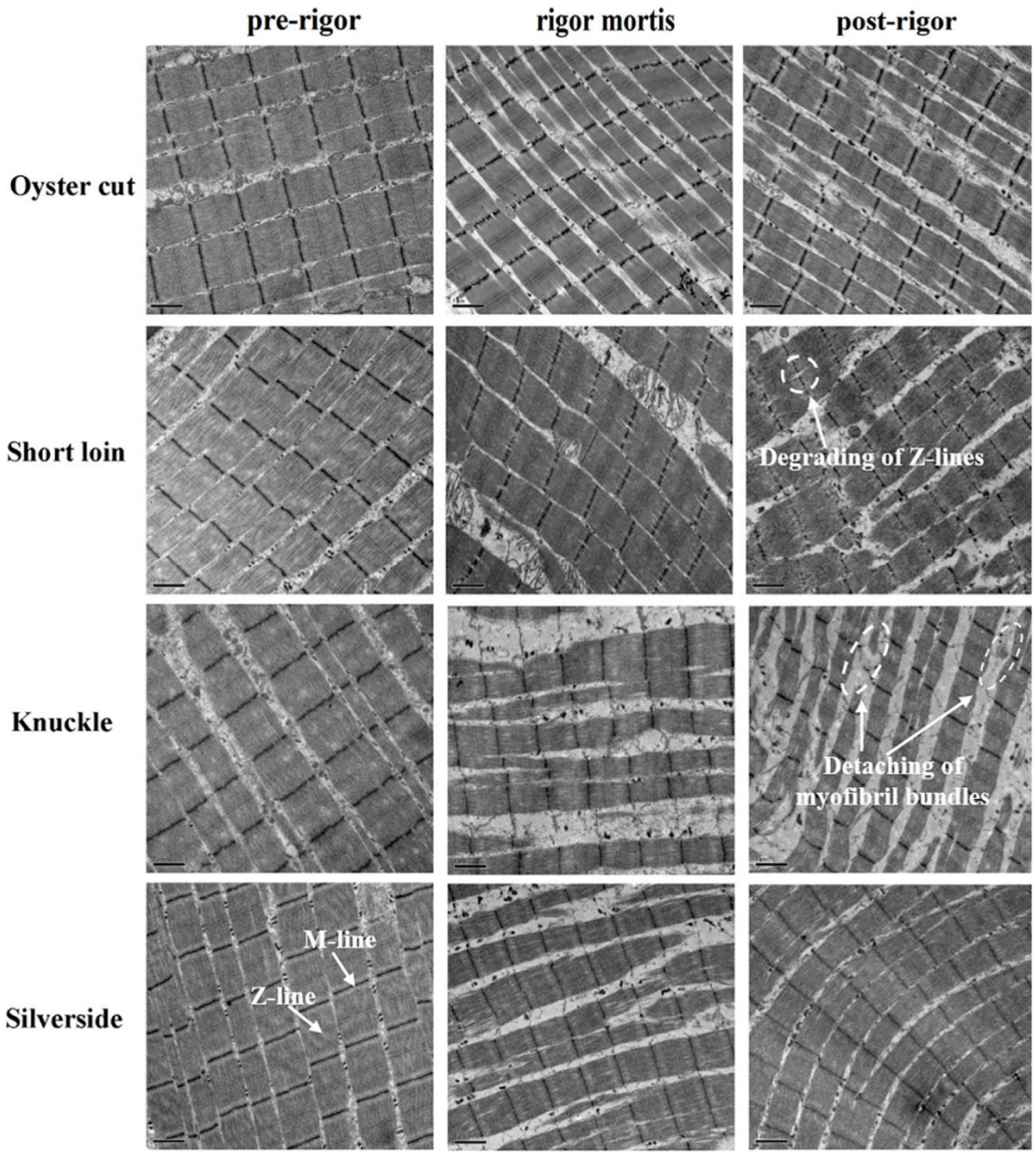

Fig. 3. Transmission electron micrographs of lamb oyster cut, short loin, knuckle and silverside in the pre-rigor, rigor mortis and post-rigor phases (15,000×). Scale bar=1 μm.

($p<0.05$, Fig. 4A). Pre-rigor cuts exhibited an intact structure and long sarcomere. During the onset of rigor mortis, the sarcomere shrank laterally and longitudinally (Fig. 3). Rigor mortis and post-rigor meat exhibited wide I-bands, dark A-bands, short sarcomeres and large inter-myofibrillar spaces. Degradation of Z-lines occurred in post-rigor cuts. From pre-rigor to post-rigor, the length of sarcomere of oyster cut, short loin, knuckle and silverside decreased from 1.57, 1.45, 1.52, 1.56 μm to 1.37, 1.20, 1.34, and 1.30 μm, respectively ($p<0.05$, Fig. 4B).

Principal component analysis (PCA)

From the result of the PCA, 62.2% of the total variability was explained by the two first principal components (PCs) with

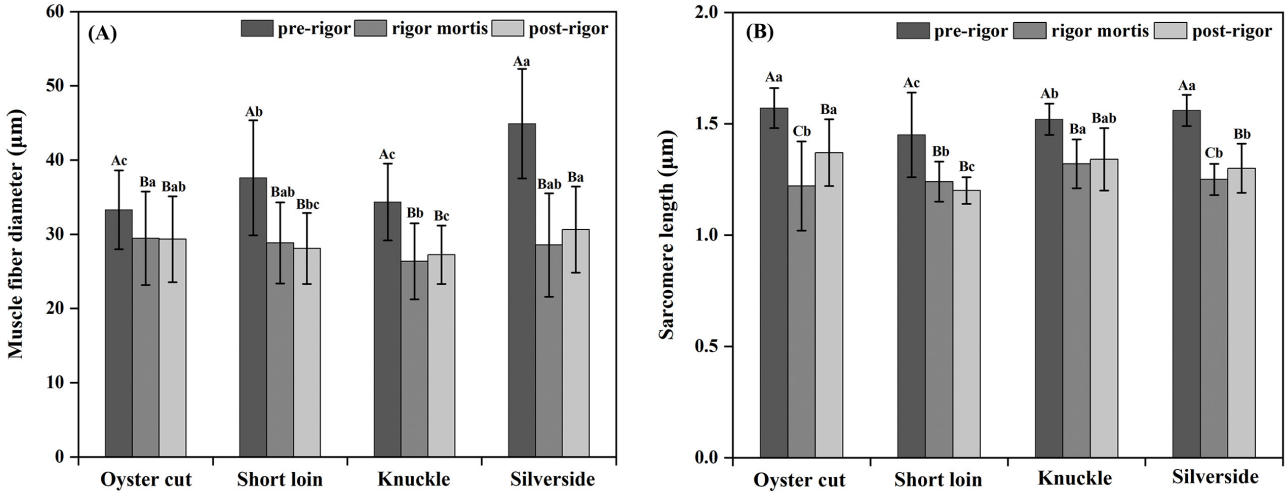

Fig. 4. Muscle fiber diameter and sarcomere length of lamb oyster cut, short loin, knuckle and silverside in the pre-rigor, rigor mortis and post-rigor phases. (A) muscle fiber diameter, (B) sarcomere length. Data were recorded as mean±SD. $^{A–C}$ Means with different letters indicate significant difference ($p<0.05$) between postmortem phases in the same cut. $^{a–c}$ Means with different letters indicate significant difference ($p<0.05$) between cuts in the same postmortem phase.

37.5% explained by PC1 and 24.7% explained by PC2. The PC1 was positively related with L*, b* and hue angle, whereas negatively related with pH. T_{21} relaxation time constant had a strongly positive influence on PC2, whereas WBSF and TL were negatively related to PC2. From the PCA score plot (Fig. 5B), there was a clear separation of pre-rigor cuts from rigor mortis and post-rigor cuts. Pre-rigor cuts were present in the negative side of PC1 characterized by higher pH and lower water loss, whereas rigor mortis and post-rigor sample were in the positive PC1 axis characterized by higher L*, b* and water loss. The score plot highlighted that rigor mortis and post-rigor cuts had similar characteristics but different from pre-rigor cuts (Fig. 5B and Figs. S1–S4).

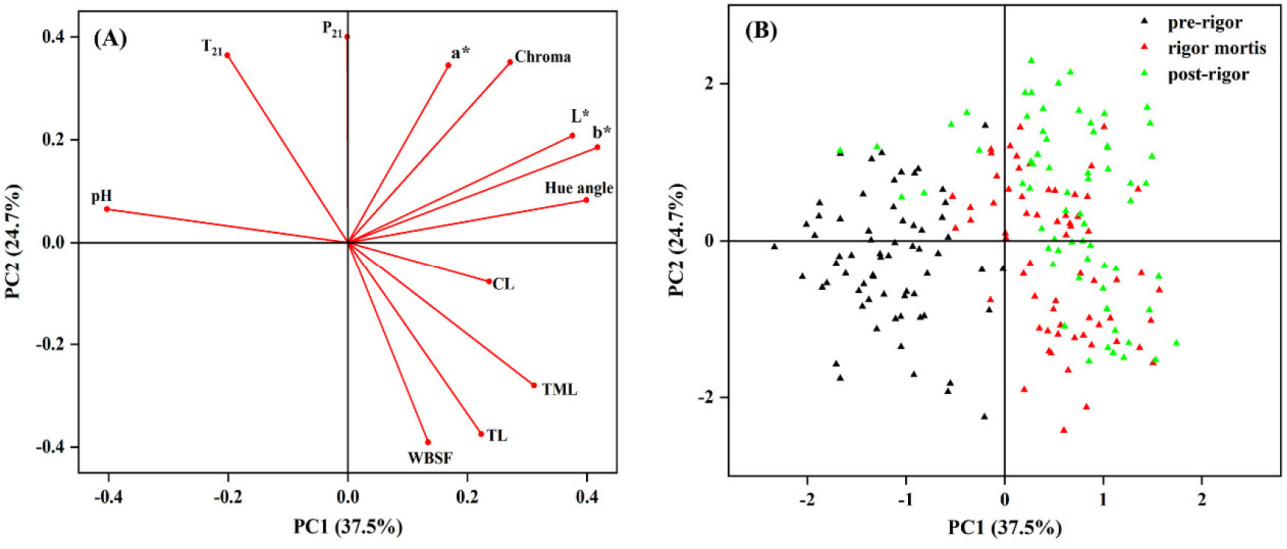

Fig. 5. Principal component analysis for meat quality parameters of lamb meat in the pre-rigor, rigor mortis and post-rigor phases. (A) loading plot, (B) score plot. CL, cooking loss; TML, total moisture loss; TL, thawing loss.

Discussion

Differential postmortem glycolysis in pre-rigor, rigor mortis and post-rigor result in different meat quality

The conversion of muscle to meat during the postmortem period involves complex energy metabolism and biochemical reaction in pre-rigor, rigor mortis and post-rigor (Lawrie and Ledward, 2017; Pearce et al., 2011). Following exsanguination, the skeletal muscle lacks the oxygen supplied to produce ATP through oxidative metabolism. Glycolysis becomes the overarching pathway to produce ATP in the postmortem period, and the accumulation of lactic acid causes pH decline and acidification of muscle (Lawrie and Ledward, 2017). Previous research studying in Poll Dorset cross-bred sheep (Ithurralde et al., 2017), Mongolian and Small-Tail Han crossbreed lamb (Xiao et al., 2020) and other lamb breeds (Geesink et al., 2011; Lawrie and Ledward, 2017) observed that the pH of lamb muscle declined from 6.5–7.0 to 5.6–6.0 during the onset of rigor mortis, and then remained stable during subsequent aging process, which were in agreement with this study. The extent and rate of pH decline postmortem could affect the WHC and color of meat (Pearce et al., 2011). In the rigor mortis phase, the pH close to the isoelectric point of myofibrillar proteins and the net charges between myofibrillar proteins decrease to near zero, which results in the less ability of myofibrillar proteins to bind water molecules and the increase of free extra-myofibrillar water within muscle (Ijaz et al., 2020). The high level of free water could be associated with the increase of water loss and the decrease of WHC (Khan et al., 2019). Under a low pH, the denaturation of sarcoplasmic proteins, as well as the increase of free water could facilitate light scattering and reflectance, which could result in the high level of L* values in rigor mortis and post-rigor cuts (Hughes et al., 2020; Ijaz et al., 2020). Dai et al. (2013) reported that the denaturation and precipitation of sarcoplasmic proteins to the myofibrils resulted in a decrease of WHC and an increase of lightness in pork *M. longissimus dorsi* muscle.

Various muscle contraction in pre-rigor, rigor mortis and post-rigor generate the variety of meat quality

Postmortem glycolysis and pH decline result in the longitudinal shortening of sarcomeres and lateral shrinkage of myofibrils (Ertbjerg and Puolanne, 2017; Hughes et al., 2020; Lana and Zolla, 2016). From pre-rigor to rigor mortis, the diameter of muscle fiber of oyster cut, short loin, knuckle and silverside decreased by 11.53%, 23.32%, 23.25%, and 36.45%, respectively; similarly, sarcomere length in those cuts decreased by 22.10%, 15.11%, 13.29%, and 19.89%, respectively. The sarcomere length of ovine *longissimus thoracis et lumborum* and bovine *semitendinosus* decreased by 24.55% Wheeler and Koohmaraie (1994) and 55.56% Stromer et al. (1967) during the onset of rigor mortis, which were in agreement with this study.

The structure of the muscle could affect the achromatic color of meat through affecting the extent of scattering, reflectance, transmission and absorption of light when the light passes through muscle fibers. The more scattering and reflection of light, meanwhile, the less absorption and transmission into the muscle structure contributing to pale meat (Hughes et al., 2020). In this study, L* values increased gradually from pre-rigor to post-rigor. Rigor mortis and post-rigor cuts had higher L* values than pre-rigor cuts. The increase of L* could be related to transverse shrinkage of muscle fibers, extracellular space formation and light scattering increase (Ertbjerg and Puolanne, 2017; Hughes et al., 2020; Pearce et al., 2011). Offer and Cousins (1992) observed that the gaps between beef *sternomandibularis* muscle fibers formed and enlarged at 24 to 48 h postmortem, which was consistent with this study. Hughes et al. (2020) reported that the shrinkage of muscle fibers had a positive effect on the increase of light scattering. Ijaz et al. (2020) reported that the increase of L* value in beef *longissimus thoracis et lumborum* during postmortem storage period might attribute to the degradation of proteins by enzymes, which caused a weaken of

protein structure and increased light dispersion. The increase of b* and hue angle values from pre-rigor to post-rigor in this study could be due to myoglobin oxidation and metmyoglobin accumulation, which was associated with brown and unattractive color of meat (Jeong et al., 2009; Suman and Joseph, 2013). Post-rigor cuts had high level of b* and hue angle values, which could cause a deviation of red hue and less desirable color of meat.

In this study, higher WBSF value was observed in rigor mortis cuts than in pre-rigor and post-rigor cuts. Sarcomere length is a critical indicator of meat tenderness, the decrease of sarcomere length leads to the increase of meat toughness (Chaosap et al., 2020). Wheeler and Koohmaraie (1994) observed that the WBSF of ovine *longissimus thoracis et lumborum* increased from 5.1 kg at 3 h postmortem to 8.66 kg at 24 h postmortem, while the sarcomere length decreased from 2.24 μm to 1.69 μm. Xiao et al. (2020) reported that the WBSF values of roasted topsides of Mongolian and Small-Tail Han crossbreed lamb increased gradually from 8.74 kg to 11.38 kg during the onset of rigor mortis and then decreased to 4.58 kg at 7 d postmortem. The shrinkage of muscle fibers was related to higher amount of myofibrillar proteins and collagen per unit area of shear therefore tough meat (Fabre et al., 2018).

Rigor mortis cuts had higher TML than pre-rigor and post-rigor cuts, the TL of rigor mortis cuts were almost twice as much as their pre-rigor counterparts in this study. The low level of WHC in rigor mortis cuts could associate with the contraction of muscle during the postmortem period. The lateral shrinkage of myofibrils as the muscle entered rigor caused a decrease of myofilament lattice spacing (Huff-Lonergan and Lonergan, 2005). The decrease of space among the myofilaments results in an expulsion of water from intra-myofibrillar to extra-myofibrillar, where the water could be easily lost from meat (Ertbjerg and Puolanne, 2017; Ijaz et al., 2020; Pearce et al., 2011). However, the degradation of cytoskeletal proteins and swelling of the muscle cells during subsequent aging could improve WHC of post-rigor cuts (Hughes et al., 2014; Pearce et al., 2011).

Distinct water states in pre-rigor, rigor mortis and post-rigor result in different meat quality

The various distribution and mobility of myowater during the conversion of muscle to meat is a possible reason of the dissimilarities of the WHC in pre-rigor, rigor mortis and post-rigor cuts (Pearce et al., 2011). In this study, rigor mortis cuts had lower T_{21} relaxation time constant and WHC compared with pre-rigor and post-rigor cuts. The proton populations of immobilized water (P_{21}) in rigor mortis oyster cut, short loin and silverside were lower than their pre-rigor and post-rigor counterparts, whereas the proton population of free water (P_{22}) increased during the onset of rigor mortis. These results were in agreement with Wu et al. (2006) who reported that the decrease of T_{21} in pork *longissimus dorsi* muscle was associated with the shrinkage of myofibrils and the loss of water. Wu et al. (2007) reported a link between WHC and T_{21} in pork meat. The higher percentage of CL, whereas lower T_{21} were observed in PSE (pale, soft, and exudative) meat than in normal and DFD (dry, firm, and dark) meat. Transverse relaxation time constant of water proton associated with the interaction between water molecules and proteins or other macromolecules in the muscle structure. Lower T_2 of proton suggests higher potential to reach a proton sink for the water molecules and lower mobility of water (Pearce et al., 2011; Shao et al., 2016). The partially shift of immobilized water to free water and repulsion from the intra-myofibrillar space to the extracellular space could be a possible reason for the low level of T_{21} and P_{21} of meat (Bertram et al., 2002; Khan et al., 2014; Wu et al., 2007). The increase of P_{22} indicates the increase of free extra-myofibrillar water in muscle (Pearce et al., 2011). It is hypothesized that the myowater volume in extra-myofibrillar space increased 1.6-fold during the onset of rigor mortis (Huff-Lonergan and Lonergan, 2005). The increase of the amount of free water within muscle resulted in an accumulation of water on the cut surface and lower WHC in rigor mortis meat than in pre-rigor meat (Devine et al., 2014).

Conclusion

Pre-rigor lamb meat had lower L*, b*, hue angle and WBSF values, whereas higher WHC than rigor mortis and post-rigor lamb meat. Oyster cut and knuckle had higher ultimate pH, L* and WHC than short loin and silverside. Distinct glycolysis, muscle contraction and water mobility could partially explain the differences of quality properties of lamb meat in different stages of postmortem. Therefore, pre-rigor lamb meat with short postmortem conditioning time had good tenderness, color and WHC. The results of this study could provide some theoretical references for lamb meat sector to produce high quality meat, meanwhile, to reduce cooler space and energy consumption and accelerate the turnover of meat.

Supplementary Materials

Supplementary materials are only available online from: https://doi.org/10.5851/kosfa.2021.e37.

Conflicts of Interest

The authors declare no potential conflicts of interest.

Acknowledgements

This research was financially supported by the Agriculture Research System (CARS-38), Key Research and Development Plan Project of Hebei Province (19227121D), and National Agricultural Science and Technology Innovation Program (CAAS-ASTIP-2021-IFST-01) in China.

Author Contributions

Conceptualization: Zhang D, Wang Z. Data curation: Ge Y, Zhang D, Zhang H, Wang Z. Formal analysis: Li X. Methodology: Ge Y, Fang F, Liang C. Software: Ge Y. Validation: Ge Y. Investigation: Ge Y, Zhang H, Liang C. Writing - original draft: Ge Y. Writing - review & editing: Ge Y, Zhang D, Zhang H, Li X, Fang F, Liang C, Wang Z.

Ethics Approval

This article does not require IRB/IACUC approval because there are no human and animal participants.

References

Bertram HC, Purslow PP, Andersen HJ. 2002. Relationship between meat structure, water mobility, and distribution: A low-field nuclear magnetic resonance study. J Agric Food Chem 50:824-829.

Calnan H, Jacob RH, Pethick DW, Gardner GE. 2016. Production factors influence fresh lamb *longissimus* colour more than muscle traits such as myoglobin concentration and pH. Meat Sci 119:41-50.

Chaosap C, Sitthigripong R, Sivapirunthep P, Pungsuk A, Adeyemi KD, Sazili AQ. 2020. Myosin heavy chain isoforms expression, calpain system and quality characteristics of different muscles in goats. Food Chem 321:126677.

Colle MJ, Richard RP, Killinger KM, Bohlscheid JC, Gray AR, Loucks WI, Day RN, Cochran AS, Nasados JA, Doumit ME. 2016. Influence of extended aging on beef quality characteristics and sensory perception of steaks from the *biceps femoris* and *semimembranosus*. Meat Sci 119:110-117.

Dai Y, Miao J, Yuan SZ, Liu Y, Li XM, Dai RT. 2013. Colour and sarcoplasmic protein evaluation of pork following water bath and ohmic cooking. Meat Sci 93:898-905.

Devine C, Wells R, Lowe T, Waller J. 2014. Pre-rigor temperature and the relationship between lamb tenderisation, free water production, bound water and dry matter. Meat Sci 96:321-326.

Ertbjerg P, Puolanne E. 2017. Muscle structure, sarcomere length and influences on meat quality: A review. Meat Sci 132:139-152.

Fabre R, Dalzotto G, Perlo F, Bonato P, Teira G, Tisocco O. 2018. Cooking method effect on Warner-Bratzler shear force of different beef muscles. Meat Sci 138:10-14.

Geesink G, Sujang S, Koohmaraie M. 2011. Tenderness of pre- and post rigor lamb *longissimus* muscle. Meat Sci 88:723-726.

Hopkins DL, Toohey ES, Warner RD, Kerr MJ, van de Ven R. 2010. Measuring the shear force of lamb meat cooked from frozen samples: Comparison of two laboratories. Anim Prod Sci 50:382-385.

Huff-Lonergan E, Lonergan SM. 2005. Mechanisms of water-holding capacity of meat: The role of postmortem biochemical and structural changes. Meat Sci 71:194-204.

Hughes JM, Clarke FM, Purslow PP, Warner RD. 2020. Meat color is determined not only by chromatic heme pigments but also by the physical structure and achromatic light scattering properties of the muscle. Compr Rev Food Sci Food Saf 19:44-63.

Hughes JM, Oiseth SK, Purslow PP, Warner RD. 2014. A structural approach to understanding the interactions between colour, water-holding capacity and tenderness. Meat Sci 98:520-532.

Ijaz M, Li X, Zhang D, Hussain Z, Ren C, Bai Y, Zheng X. 2020. Association between meat color of DFD beef and other quality attributes. Meat Sci 161:107954.

Ithurralde J, Bianchi G, Feed O, Nan F, Ballesteros F, Garibotto G, Bielli A. 2017. Variation in instrumental meat quality among 15 muscles from 14-month-old sheep and its relationship with fibre typing. Anim Prod Sci 58:1358-1365.

Jeong JY, Hur SJ, Yang HS, Moon SH, Hwang YH, Park GB, Joo ST. 2009. Discoloration characteristics of 3 major muscles from cattle during cold storage. J Food Sci 74:C1-C5.

Khan MA, Ali S, Abid M, Cao J, Jabbar S, Tume RK, Zhou G. 2014. Improved duck meat quality by application of high pressure and heat: A study of water mobility and compartmentalization, protein denaturation and textural properties. Food Res Int 62:926-933.

Khan MA, Ali S, Yang H, Kamboh AA, Ahmad Z, Tume RK, Zhou G. 2019. Improvement of color, texture and food safety of ready-to-eat high pressure-heat treated duck breast. Food Chem 277:646-654.

Kim YHB, Ma D, Setyabrata D, Farouk MM, Lonergan SM, Huff-Lonergan E, Hunt MC. 2018. Understanding postmortem biochemical processes and post-harvest aging factors to develop novel smart-aging strategies. Meat Sci 144:74-90.

Lana A, Zolla L. 2016. Proteolysis in meat tenderization from the point of view of each single protein: A proteomic perspective. J Proteomics 147:85-97.

Lang Y, Sha K, Zhang R, Xie P, Luo X, Sun B, Li H, Zhang L, Zhang S, Liu X. 2016. Effect of electrical stimulation and hot boning on the eating quality of Gannan yak *longissimus lumborum*. Meat Sci 112:3-8.

Lawrie RA, Ledward DA. 2017. Lawrie's meat science. Woodhead, Abington, UK. pp 159-381.

Li C, Liu D, Zhou G, Xu X, Qi J, Shi P, Xia T. 2012. Meat quality and cooking attributes of thawed pork with different low field NMR T_{21}. Meat Sci 92:79-83.

Li FK, Yang Y, Jenna K, Xia CH, Lv SJ, Wei WH. 2018. Effect of heat stress on the behavioral and physiological patterns of Small-tail Han sheep housed indoors. Trop Anim Health Prod 50:1893-1901.

Li X, Zhang D, Ren C, Bai Y, Ijaz M, Hou C, Chen L. 2021. Effects of protein posttranslational modifications on meat quality: A review. Compr Rev Food Sci Food Saf 20:289-331.

Li Y, Li X, Wang J, Zhang C, Sun H, Wang C, Xie X. 2014. Effects of oxidation on water distribution and physicochemical properties of porcine myofibrillar protein gel. Food Biophys 9:169-178.

Nam KC, Jo C, Lee M. 2010. Meat products and consumption culture in the East. Meat Sci 86:95-102.

Offer G, Cousins T. 1992. The mechanism of drip production: Formation of two compartments of extracellular space in muscle post mortem. J Sci Food Agric 58:107-116.

Pearce KL, Rosenvold K, Andersen HJ, Hopkins DL. 2011. Water distribution and mobility in meat during the conversion of muscle to meat and ageing and the impacts on fresh meat quality attributes: A review. Meat Sci 89:111-124.

Qian S, Li X, Wang H, Wei X, Mehmood W, Zhang C, Blecker C. 2020. Contribution of calpain to protein degradation, variation in myowater properties and the water-holding capacity of pork during postmortem ageing. Food Chem 324:126892.

Shao JH, Deng YM, Song L, Batur A, Jia N, Liu DY. 2016. Investigation the effects of protein hydration states on the mobility water and fat in meat batters by LF-NMR technique. LWT-Food Sci Technol 66:1-6.

Stromer MH, Goll DE, Roth LE. 1967. Morphology of rigor-shortened bovine muscle and the effect of trypsin on pre- and postrigor myofibrils. J Cell Biol 34:431-445.

Sukumaran AT, Holtcamp AJ, Campbell YL, Burnett D, Schilling MW, Dinh TTN. 2018. Technological characteristics of pre- and post-rigor deboned beef mixtures from Holstein steers and quality attributes of cooked beef sausage. Meat Sci 145:71-78.

Suleman R, Wang Z, Aadil RM, Hui T, Hopkins DL, Zhang D. 2020. Effect of cooking on the nutritive quality, sensory properties and safety of lamb meat: Current challenges and future prospects. Meat Sci 167:108172.

Suman SP, Joseph P. 2013. Myoglobin chemistry and meat color. Annu Rev Food Sci Technol 4:79-99.

Wheeler TL, Koohmaraie M. 1994. Prerigor and postrigor changes in tenderness of ovine *longissimus muscle*. J Anim Sci 72:1232-1238.

Wu JY, Mills EW, Henning WR. 1995. Postmortem delay time and heating rate affect tenderness and ultrastructure of prerigor cooked bovine muscle. J Food Sci 60:565-570.

Wu Z, Bertram HC, Böcker U, Ofstad R, Kohler A. 2007. Myowater dynamics and protein secondary structural changes as affected by heating rate in three pork qualities: A combined FT-IR microspectroscopic and ^{1}H NMR relaxometry study. J Agric Food Chem 55:3990-3997.

Wu Z, Bertram HC, Kohler A, Böcker U, Ofstad R, Andersen HJ. 2006. Influence of aging and salting on protein secondary structures and water distribution in uncooked and cooked pork. A combined FT-IR microspectroscopy and ^{1}H NMR relaxometry study. J Agric Food Chem 54:8589-8597.

Xiao X, Hou C, Zhang D, Li X, Ren C, Ijaz M, Hussain Z, Liu D. 2020. Effect of pre- and post-rigor on texture, flavor, heterocyclic aromatic amines and sensory evaluation of roasted lamb. Meat Sci 169:108220.